3 Reactions of $[RuCl_2(depe)_2]$

3.1 Introduction

The ligand 1,2-*bis*(diethylphosphino)ethane (depe), whilst having an overall chemistry that is very similar to dmpe, has some differences that are occasionally manifested in the reactivity of the overall complex. For example, the compound $[FeCl_2(dmpe)_2]$ dissolves in alcohols under N_2 to form $[FeCl(N_2)(dmpe)_2]^+$, which may be isolated as its tetraphenylborate salt by addition of $NaBPh_4$, however, when the analogous reaction is attempted for $[FeCl_2(depe)_2]$, the solid isolated does indeed give a strong ν_{NN}, but the nitrogen content varies from preparation to preparation and is always less than 1:1.[1]

In metal complexes, the chelating depe ligand is frequently observed to be more labile than dmpe,[2] leading to effects such as increased susceptibility to protonation and a lower energy barrier to isomerisation. Additionally, the ethyl substituents are more likely to cyclometallate a coordinatively unsaturated metal centre when compared with dmpe.[3]

3.2 Reactions of trans-[$RuCl_2(depe)_2$]

3.2.1 Treatment of *trans*-[$RuCl_2(depe)_2$] with Ag(OTf) in dichloromethane

T*rans*-[$RuCl_2(depe)_2$] was synthesised analogously to *trans*-[$RuCl_2(dmpe)_2$] (Chapter 2, Section 2.2).

Unlike the reaction of *trans*-[$RuCl_2(dmpe)_2$] with silver triflate in dichloromethane (Chapter 2, Section 2.5.1), the reaction of *trans*-[$RuCl_2(depe)_2$] with Ag(OTf) under analogous conditions resulted in the formation of a complex mixture of diamagnetic products, together with development of the characteristic blue colour of ruthenium(III) complexes. The observation of diamagnetic and paramagnetic products from the one reaction is likely to be caused by kinetic competition between chloride abstraction and ruthenium oxidation, with the large number of diamagnetic products observed arising from coordinatively unsaturated species formed *via* chloride abstraction reacting with dichloromethane to form a mix of species.

3.2.2 Treatment of *trans*-[$RuCl_2(depe)_2$] with TMS(OTf) in toluene

The reaction of [$RuCl_2(depe)_2$] with TMS(OTf) in toluene proceeds analogously to the dmpe reaction, forming the ruthenium(III) complex *trans*-[$RuCl_2(depe)_2$](OTf) (Scheme 3.1).

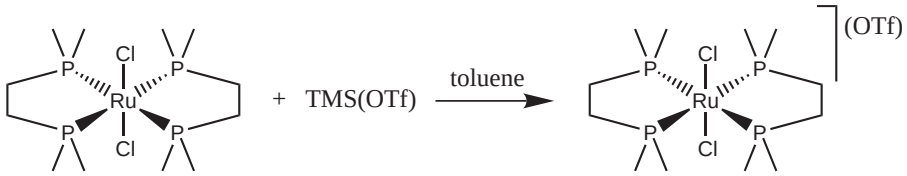

Scheme 3.1

The complex exhibits a ^1H NMR spectrum with paramagnetically shifted alkyl resonances (Figure 3.1) similar to those in the spectrum of *trans*-$[RuCl_2(dmpe)_2](OTf)$ (Chapter 2, Section 2.5.1). The methyl portions of the ethyl substituents are sufficiently distant from the metal centre to show only a marginal shift and minimal broadening.

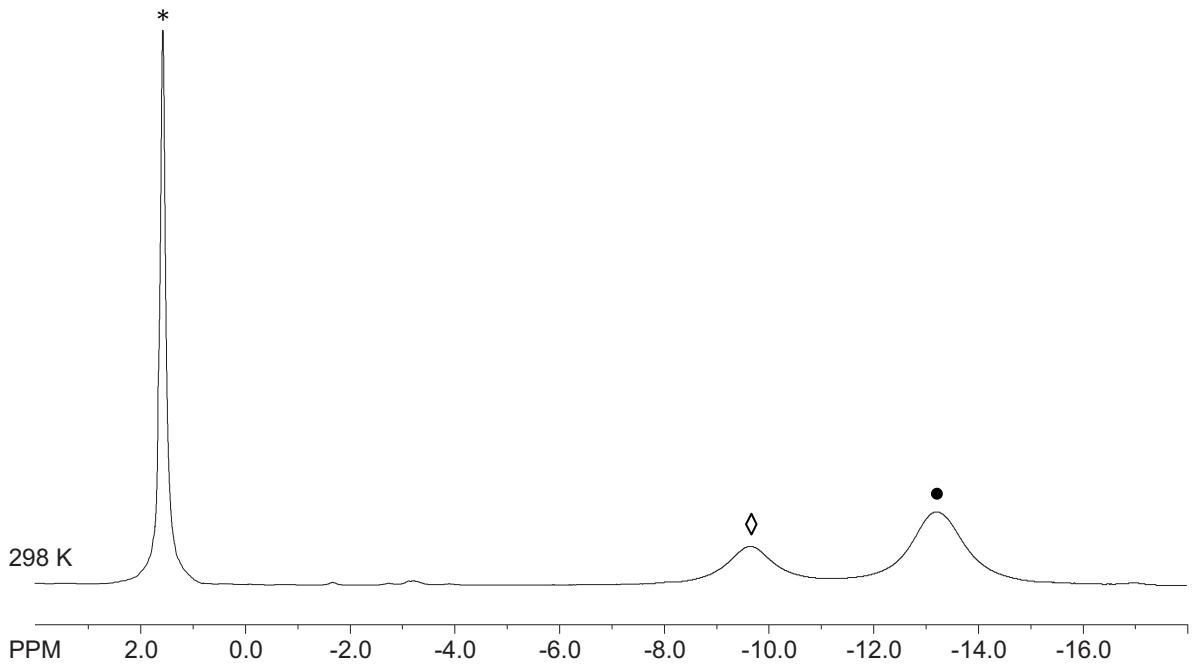

Figure 3.1 – $^1H\{^{31}P\}$ NMR spectrum (d_8-thf, 400 MHz) of *trans*-$[RuCl_2(depe)_2](OTf)$, displaying paramagnetically shifted methylene (●) and ethylene (◊) proton resonances, along with the non-shifted terminal methyl resonance (*)

3.2.3 Treatment of *trans*-[$RuCl_2(depe)_2$] with Tl(OTf) in tetrahydrofuran

Reaction of [$RuCl_2(depe)_2$] with thallium triflate in tetrahydrofuran heated at reflux generated a white precipitate and a thermochromic solution which was initially orange and transitioned through yellow and green upon cooling before stabilising as a dark green (almost black) solution that yielded a dark green solid upon solvent removal. The product was soluble in acetone, methanol, and dichloromethane and moderately soluble in tetrahydrofuran, however it was insoluble in benzene or toluene, instead forming an immiscible oil such that the complex could pass through a fine sintered glass frit when such a mixture was filtered.

The $^{31}P\{^{1}H\}$ NMR spectrum at 300 K consists of two broad apparent triplets at 62.1 and 45.9 ppm characteristic of a *cis* symmetrical complex, and two broader resonances at 66.1 and 48.8 ppm. The resonances in the downfield region (66.1 and 62.1 ppm) are associated with the equatorial phosphine positions of *cis* complexes with ionic co-ligands (such as chloride) *trans* to the phosphine atoms, whilst the resonances in the upfield region (48.8 and 45.9 ppm) are associated with the axial phosphine positions of *cis* complexes.

Cooling the NMR sample down to 270 K results in sharpening of the *cis* symmetrical complex resonances into two well-resolved apparent

triplets, whilst further cooling to 210 K results in eventual resolution of the remaining broad resonances into the characteristic AMXY pattern of an unsymmetrically substituted *cis* complex. The equatorial phosphine resonances of this species have very similar chemical shifts such that the spin system is approaching ABXY in nature. A stacked plot of the variable temperature $^{31}P\{^{1}H\}$ NMR experiments is shown in Figure 3.2.

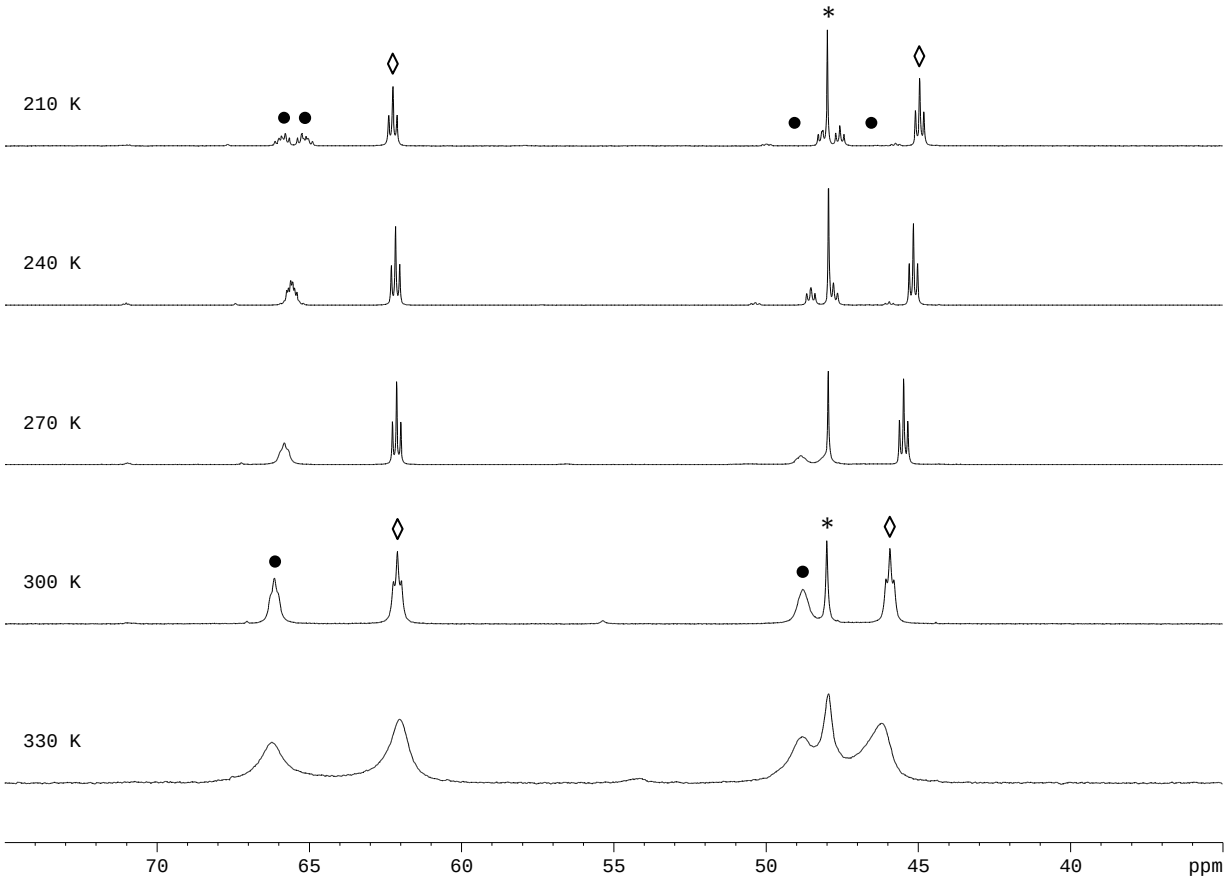

Figure 3.2 – Variable temperature $^{31}P\{^{1}H\}$ NMR spectra (d_8-thf, 162 MHz) of the product formed in the reaction of *trans*-$[RuCl_2(depe)_2]$ with thallium triflate. ◊ – *cis*-$[\{Ru(depe)_2\}_2(\mu\text{-}Cl)_2](OTf)_2$; ● – *cis*-$[RuCl(OTf)(depe)_2]$; * – Starting material

EXSY (EXchange SpectroscopY) is an NMR technique that is the 2D analogue of a saturation transfer experiment.[4,5] By employing ^{31}P-^{31}P EXSY (at 300 K) to probe the exchange processes in solution, a strong correlation was observed between the upfield resonances at 48.8 and 45.9 ppm as well as between the downfield resonances at 66.1 and 62.1 ppm. Weaker correlations were observed between the upfield and downfield resonances, indicating a high degree of exchange occurring between the species in solution (Figure 3.3).

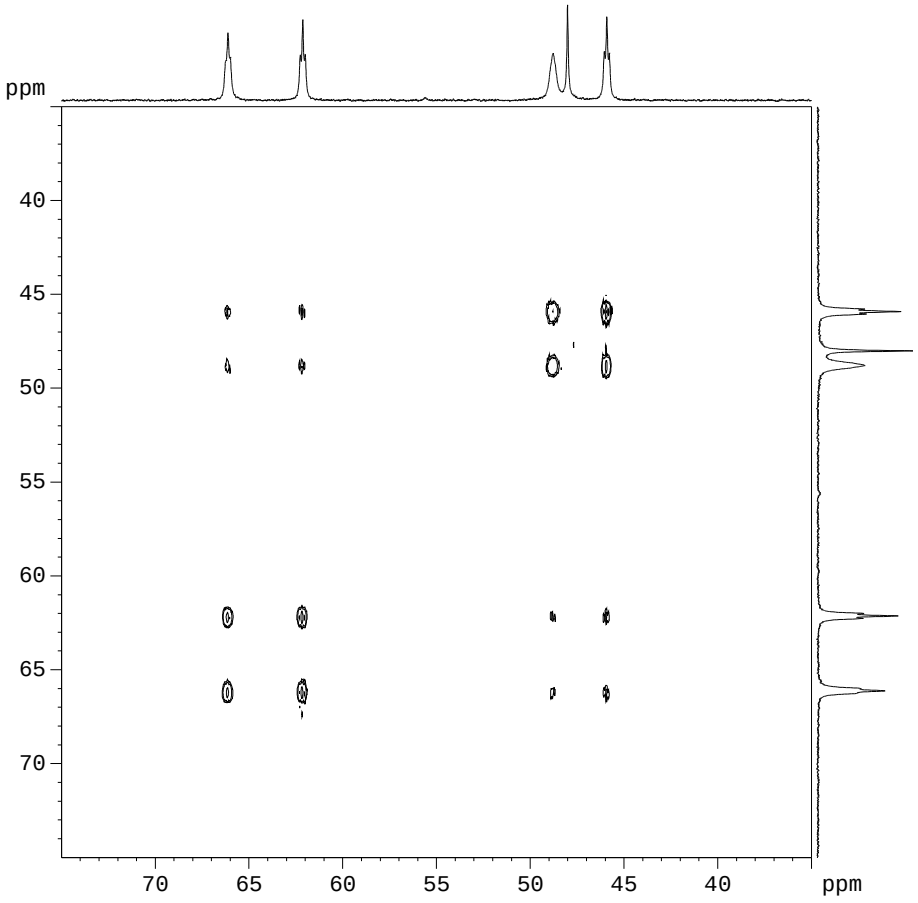

Figure 3.3 – ^{31}P-^{31}P EXSY spectrum (d_8-thf, 162 MHz, mixing time = 1.5 s) at 300 K

At temperatures below 270 K all observable exchange, at the EXSY mixing time of 1.5 s, ceases. On the basis of the combined NMR data it is apparent that there are two *cis* complexes in solution and that there is dynamic exchange between the two.

MALDI-MS of the mixture reveals only three fragment ions at *m/z* 549, 584, and 1098. The low molecular weight ions have *m/z* ratios and isotopic distribution patterns indicative of $[RuCl(depe)_2]^+$ and $[RuCl_2(depe)_2]^+$ respectively, whilst the ion fragment at *m/z* 1098 has a complicated isotopic distribution pattern that suggests at least two ruthenium atoms. Using molecular mass calculations and isotopic modelling, the closest fragment ion match is the formula $[Ru_2Cl_2(depe)_4]^+$ (Figure 3.4).

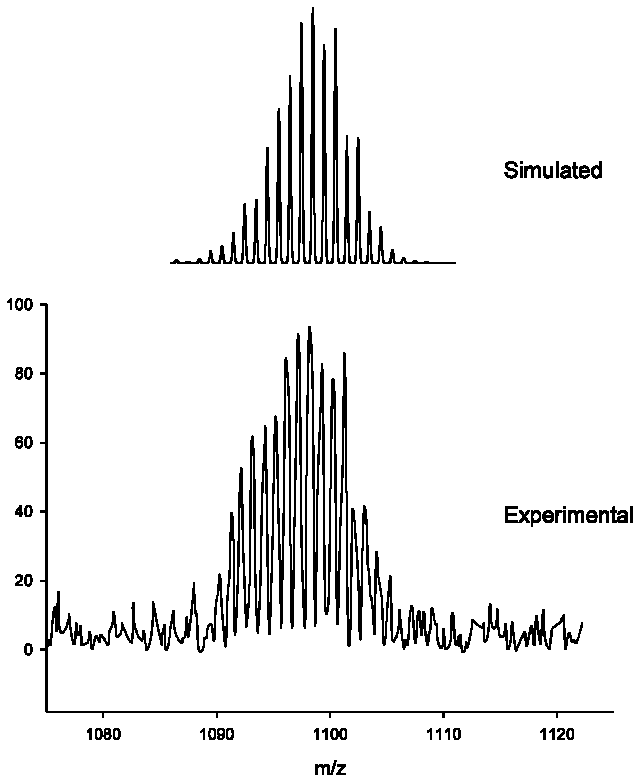

Figure 3.4 – Experimental and simulated ion envelopes of $[Ru_2Cl_2(depe)_4]^+$

On the basis of the above information, the reaction product is proposed to be a mixture of a doubly chloride-bridged dimer, *cis*-$[\{Ru(depe)_2\}_2(\mu\text{-}Cl)_2](OTf)_2$, which is in equilibrium with a monomeric form containing a weakly coordinating triflate, *i.e.*, *cis*-$[RuCl(OTf)(depe)_2]$ (Scheme 3.2), though the latter may more correctly be assigned as *cis*-$[RuCl(depe)_2]^+$ on the basis of the formation of an identical product when $Tl(BF_4)$ was used in place of Tl(OTf) (Section 3.3.3).

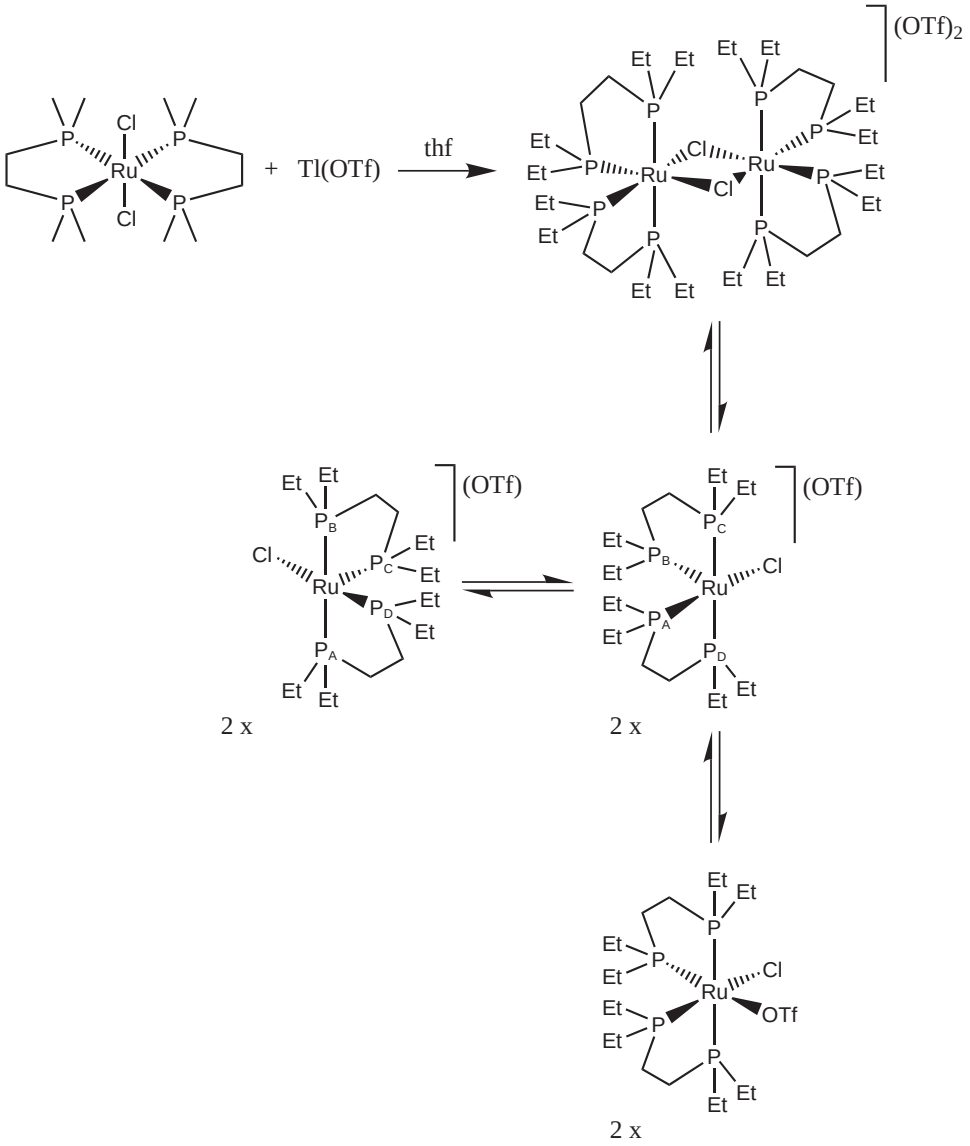

Scheme 3.2

A dimeric structure in which the ruthenium centres are bridged by one or more depe molecules rather than two chloride ligands is ruled out due to a number of factors, the most important of which is the ^{31}P chemical shift of the depe ligands, which are consistent with the significant downfield shift that 5-membered chelate rings display.[6] A depe bridged structure would also require additional ligands to fill the coordination

sphere of each ruthenium, which, whilst not impossible, would be expected to be observed *via* MS or NMR spectroscopy.

There is significant evidence to suggest that the chloride-bridged dimer is stabilised by thallium in a manner similar to $Tl[\{Ru(C{\equiv}C^tBu)(dcypb)\}_2(\mu\text{-}Cl)_3]$.[7] Evidence that supports the incorporation of thallium into the complex includes the observation that reacting the product with a variety of donor ligands resulted in precipitation of a white solid, presumably TlCl, and that the ratio of *cis*-$[\{Ru(depe)_2\}_2(\mu\text{-}Cl)_2](OTf)_2$ to *cis*-$[RuCl(OTf)(depe)_2]$ varied from preparation to preparation, which is consistent with the idea that *cis*-$[\{Ru(depe)_2\}_2(\mu\text{-}Cl)_2](OTf)_2$ can be more accurately described as *cis*-$[\{Ru(depe)_2\}_2(\mu\text{-}\eta^4\text{-}Cl)_2(Tl)_2](OTf)_2$ (Figure 3.5). Furthermore, MALDI-MS run without the presence of a matrix (C_{60}) gives rise to a series of thallium-chloride clusters of the form Tl_nCl_{n-1}. The variable incorporation of thallium in such a manner goes some way to explaining why it has not yet been possible to obtain reliable microanalytical data for this species.

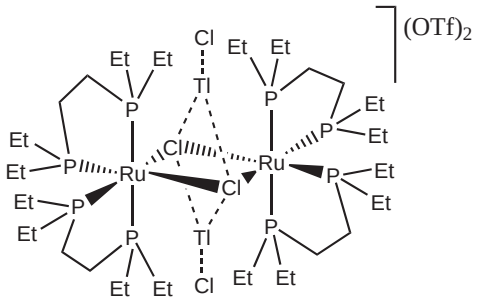

Figure 3.5 – Representation of thallium-stabilised *cis*-$[\{Ru(depe)_2\}_2(\mu\text{-}Cl)_2](OTf)_2$

Closer inspection of the $^{31}P\{^{1}H\}$ NMR spectrum reveals a small resonance at 48 ppm belonging to a *trans* complex, that although somewhat fluxional at ambient temperature, does not exchange with any of the other species in solution. On the basis of a lack of observable dinitrogen stretches in the IR spectrum, no unaccounted-for fragments in MALDI-MS spectra, and the mild fluxionality displayed by this species, the complex is most likely to be *trans*-[$RuCl(OTf)(depe)_2$] or a thallium adduct of the form *trans*-[$RuCl_2(depe)_2$]·Tl(OTf), as per the analogous reaction with *trans*-[$RuCl_2(dmpe)_2$] (Chapter 2, Section 2.5.3).

3.2.4 Reactions of *cis*-[{$Ru(depe)_2$}$_2$(μ-$Cl)_2$]$(OTf)_2$

Reaction of *cis*-[{$Ru(depe)_2$}$_2$(μ-$Cl)_2$]$(OTf)_2$ with sodium tetraphenylborate in ethanol resulted in precipitation of a light green-grey solid which contained a multitude of species as observed by ^{31}P NMR spectroscopy. IR spectroscopy confirms that at least one of the species formed contains a terminally coordinated dinitrogen, as there is a significant dinitrogen stretch at 2127 cm^{-1}. C*is*-[{$Ru(depe)_2$}$_2$(μ-$Cl)_2$]$(OTf)_2$ also reacted with a variety of neutral donor ligands and nucleophiles, and such reactions are elaborated upon in Chapter 4.

3.2.5 Treatment of *trans*-$[RuCl_2(depe)_2]$ with TMS(OTf) in methanol

Variation of the solvent from toluene to methanol in the reaction of *trans*-$[RuCl_2(depe)_2]$ with trimethylsilyl triflate afforded, along with a minor product contributing to four broad $^{31}P\{^1H\}$ resonances, a dominant product that displays highly fluxional behaviour. Even at 198 K, the fluxional species appears as two broad signals in the ^{31}P NMR spectrum, *ca.* 60 Hz wide. IR spectroscopy reveals no ν_{NN} signals, and MALDI-MS contains ion envelopes for $[RuCl(depe)_2]^+$ and $[RuCl_2(depe)_2]^+$ only. Overall the reaction mixture appears to be spectroscopically similar to the *cis*-$[\{Ru(depe)_2\}_2(\mu\text{-}Cl)_2](OTf)_2$ / *cis*-$[RuCl(OTf)(depe)_2]$ system (Section 3.2.3), albeit much more fluxional.

One likely explanation for the increased fluxionality is the lack of thallium in the system, as thallium appeared to stabilise the doubly chloride-bridged dimer and presumably slowed down the rate of exchange between *cis*-$[\{Ru(depe)_2\}_2(\mu\text{-}Cl)_2](OTf)_2$ and the monomeric *cis*-$[RuCl(OTf)(depe)_2]$ to a level where such species were clearly observable on the NMR timescale. Supporting this hypothesis is the small signal for $[Ru_2Cl_2(depe)_4]^+$ at *m/z* 1098 in MALDI-MS spectra recorded at high laser power. At higher laser power, fragmentation ions become a problem and detector saturation becomes significant, resulting in extremely distorted ion envelopes. Nevertheless, such laser powers

are frequently required to observe high molecular mass species and can be useful for observation of compounds that are difficult to ionise.

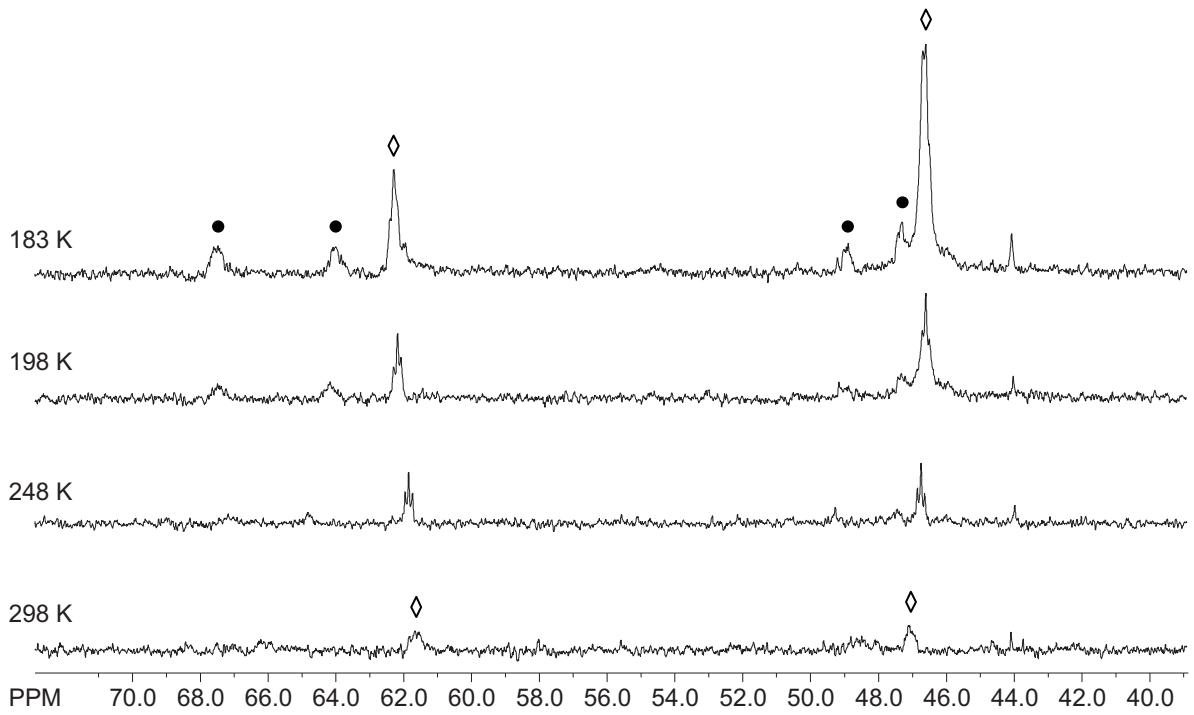

Figure 3.6 – Variable temperature $^{31}P\{^1H\}$ NMR spectra (d_8-thf, 202 MHz) of the reaction mixture of *trans*-$[RuCl_2(depe)_2]$ + TMS(OTf). ◊ – *cis*-$[\{Ru(depe)_2\}_2(\mu\text{-}Cl)_2](OTf)_2$; ● – *cis*-$[RuCl(OTf)(depe)_2]$

3.2.6 Treatment of *trans*-$[RuCl_2(depe)_2]$ with Ag(OTf) in methanol

Reaction of *trans*-$[RuCl_2(depe)_2]$ with silver triflate in methanol heated at reflux under an atmosphere of dinitrogen resulted in precipitation of a fine grey solid and formation of a green solution that slowly turned yellow upon cooling. Filtration followed by removal of the solvent *in vacuo* gave a yellow solid that became dark green (over several days) when stored under dinitrogen. The product is only sparingly soluble in

tetrahydrofuran, hence NMR spectra were recorded in $CDCl_3$. The $^{31}P\{^1H\}$ NMR spectrum of the complex reveals an unusual spin system best represented by AA´MM´XX´, where the AA´ and MM´ spins are the standard equatorial and axial resonances of a symmetrically substituted *cis*-diphosphine complex that give rise to two apparent triplets, and XX´ belongs to a non-phosphorus spin-½ nucleus that couples only to the axial phosphorus atoms with a P-X coupling constant of approximately 7.7 Hz.

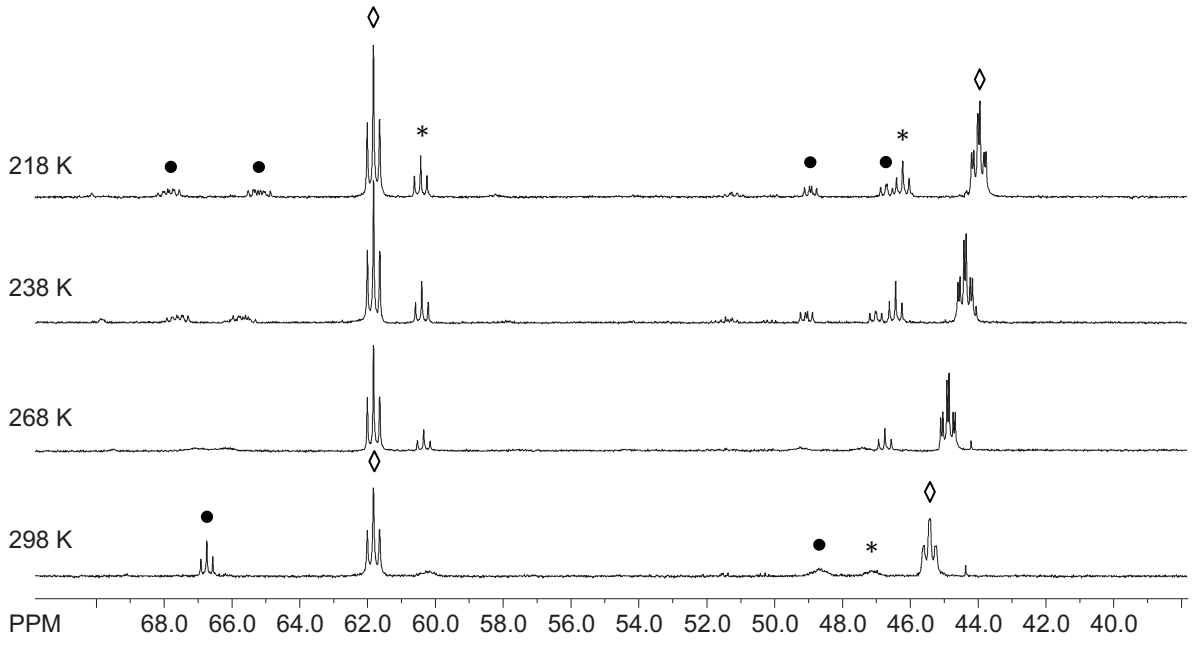

Figure 3.7 – Variable temperature $^{31}P\{^1H\}$ NMR spectra ($CDCl_3$, 121 MHz) of the reaction mixture of *trans*-$[RuCl_2(depe)_2]$ + Ag(OTf) . ◊ – 'Silver-stabilised' *cis*-$[\{Ru(depe)_2\}_2(\mu\text{-}Cl)_2](OTf)_2$; ● – unknown *cis* unsymmetrical; * – 'Unstabilised' *cis*-$[\{Ru(depe)_2\}_2(\mu\text{-}Cl)_2](OTf)_2$

The only nuclei of I = ½ which could be potential additional ligands in the system are ^1H, abstracted from methanol or adventitious water, ^{19}F, abstracted from a triflate anion, or Ag, which has two spin-½ isotopes

(^{107}Ag and ^{109}Ag) that total 100% abundance (51.8 and 48.2 % respectively). No evidence of metal-hydride species were observed, nor of abstracted fluoride.

A symmetrical, dimeric structure is required to account for the observed spin systems and the MALDI-MS ion envelopes of *m/z* 549 ($[RuCl(depe)_2]^+$) and *m/z* 1098 ($[Ru_2Cl_2(depe)_4]^+$). Therefore evidence points towards a silver-stabilised ruthenium dimer, probably of the form *cis*-$[\{Ru(depe)_2\}_2(\mu\text{-}Cl)_2](OTf)_2 \cdot 2Ag(Cl)$ (Figure 3.8), analogous to the thallium-stabilised adduct proposed in Section 3.2.1. In such a complex, the bridging silver atoms may display coupling to the axial phosphine groups.

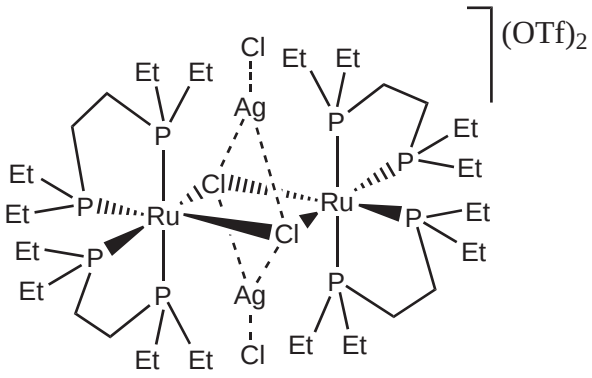

Figure 3.8 – Representation of silver-stabilised *cis*-$[\{Ru(depe)_2\}_2(\mu\text{-}Cl)_2](OTf)_2$

Also present as a minor species in the $^{31}P\{^1H\}$ NMR spectrum is a symmetrically substituted *cis* complex with two apparent triplets at *ca*. 60 and 47 ppm. The resonances corresponding to this species are broad at ambient temperature, yet gradually sharpen as the temperature is

decreased to 268 K. One plausible assignment is as an 'unstabilised' dimer of the form *cis*-$[\{Ru(depe)_2\}_2(\mu\text{-}Cl)_2](OTf)_2$, where the lack of a stabilising 'bridging' metal results in a significantly greater degree of fluxionality. The similarity in chemical shifts of this species to the product formed in the reaction between *trans*-$[RuCl_2(depe)_2]$ with TMS(OTf) in methanol (Section 3.2.5) supports this assignment.

It is of interest that, unlike *cis*-$[\{Ru(depe)_2\}_2(\mu\text{-}Cl)_2](OTf)_2 \cdot 2Tl(Cl)$, $^{31}P\{^1H\}$ NMR spectra of *cis*-$[\{Ru(depe)_2\}_2(\mu\text{-}Cl)_2](OTf)_2 \cdot 2Ag(Cl)$ are remarkably sharp at all temperatures and do not show any species that may be interpreted as the monomeric form. This suggests that silver is significantly more efficient at stabilising the doubly chloride-bridged ruthenium dimer, minimising the propensity of the dimer to cleave into a monomeric form. Whilst the use of both silver and thallium salts in chloride abstraction are reported to often result in the formation of Ru-Cl-M adducts,[8] it is interesting to note the differences between these two metals.

3.2.7 Treatment of *trans*-$[RuCl_2(depe)_2]$ with $Tl(BArF_{24})$ in methanol

Reaction of *trans*-$[RuCl_2(depe)_2]$ with $Tl(BArF_{24})$ in methanol at ambient temperature resulted in precipitation of a white solid and the formation of a yellow solution. Filtration followed by removal of the solvent *in*

vacuo resulted in the formation of a yellow solid that slowly turned green when stored under a dinitrogen atmosphere.

MALDI-MS of the green species reveals the presence of $[RuCl(depe)_2]^+$ at *m/z* 549 and a minor (*ca.* 10%) ion envelope at *m/z* 577, assignable as $[RuCl(N_2)(depe)_2]^+$. The IR spectrum contains only CH and fingerprint vibrations, whilst Raman spectroscopy was unsuccessful due to sample decomposition.

The $^{31}P\{^1H\}$ NMR spectrum exhibits a well resolved AMXZ spin system at all temperatures between 298 and 198 K, with the chemical shift difference between equatorial phosphine groups being some 9.7 ppm at 202 MHz. The axial phosphine groups have a chemical shift difference of 2 ppm and a coupling constant of 227 Hz to each other, leading to deviation from first order behaviour that manifests as tenting (Figure 3.9). The significantly larger chemical shift differences in this system relative to previous unsymmetrically substituted *cis* complexes must arise as a function of the differences in bonding/back-bonding properties between the two equatorial co-ligands, *i.e.*, between the chloride ligand and the unknown neutral ligand that coordinates to Ru^{II} upon initial chloride abstraction. Despite a lack of confirmation *via* vibrational spectroscopy, a consideration of the MALDI-MS data and the reaction conditions suggests that the unknown neutral ligand is coordinated dinitrogen, which is most likely coordinated in a bridging fashion.

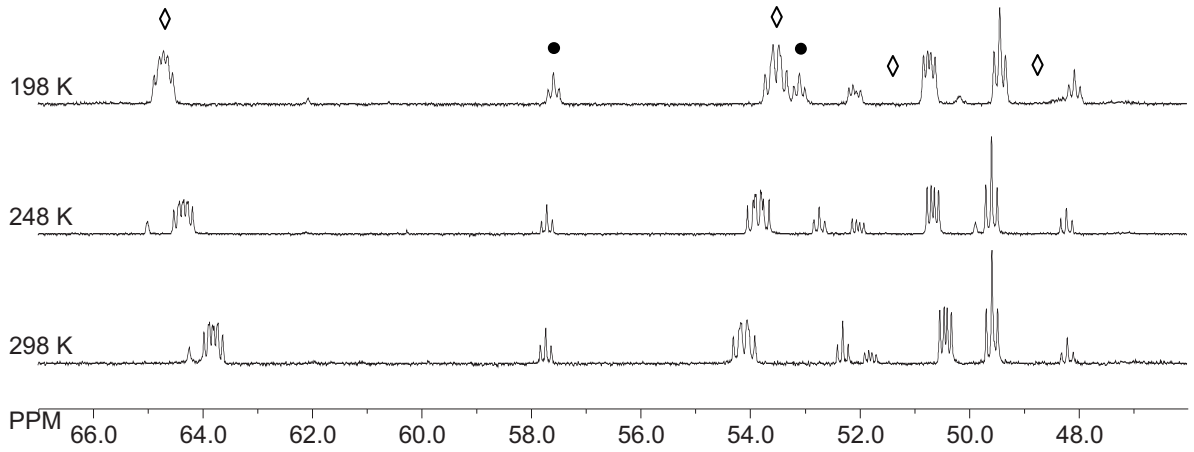

Figure 3.9 – Variable temperature $^{31}P\{^1H\}$ NMR spectra (d_8-thf, 202 MHz) of the reaction mixture of *trans*-$[RuCl_2(depe)_2]$ + $Tl(BArF_{24})$. ◊ – *cis*-$[\{RuCl(depe)_2\}_2(\mu\text{-}N_2)](BArF_{24})_2$; ● – unknown *cis* symmetrical

Crystallisation *via* slow diffusion of heptane over several weeks into a dichloromethane solution of the reaction product under an atmosphere of dinitrogen resulted in the formation of small, blue, monoclinic ($P2_1/c$) crystals. In view of the low quality of the crystal data and the limitations of X-ray analysis, it is not possible to unambiguously distinguish the putative dinitrogen complex from an alternative carbonyl-containing species. However, given that the crude reaction mixture had been shown spectroscopically to not contain CO and the low likelihood that carbon monoxide was introduced or generated in the process of crystallisation, preliminary X-ray structural analysis allows identification of the crystallised species as *trans*-$[RuCl(N_2)(depe)_2](BArF_{24})$ (Figure 3.10).

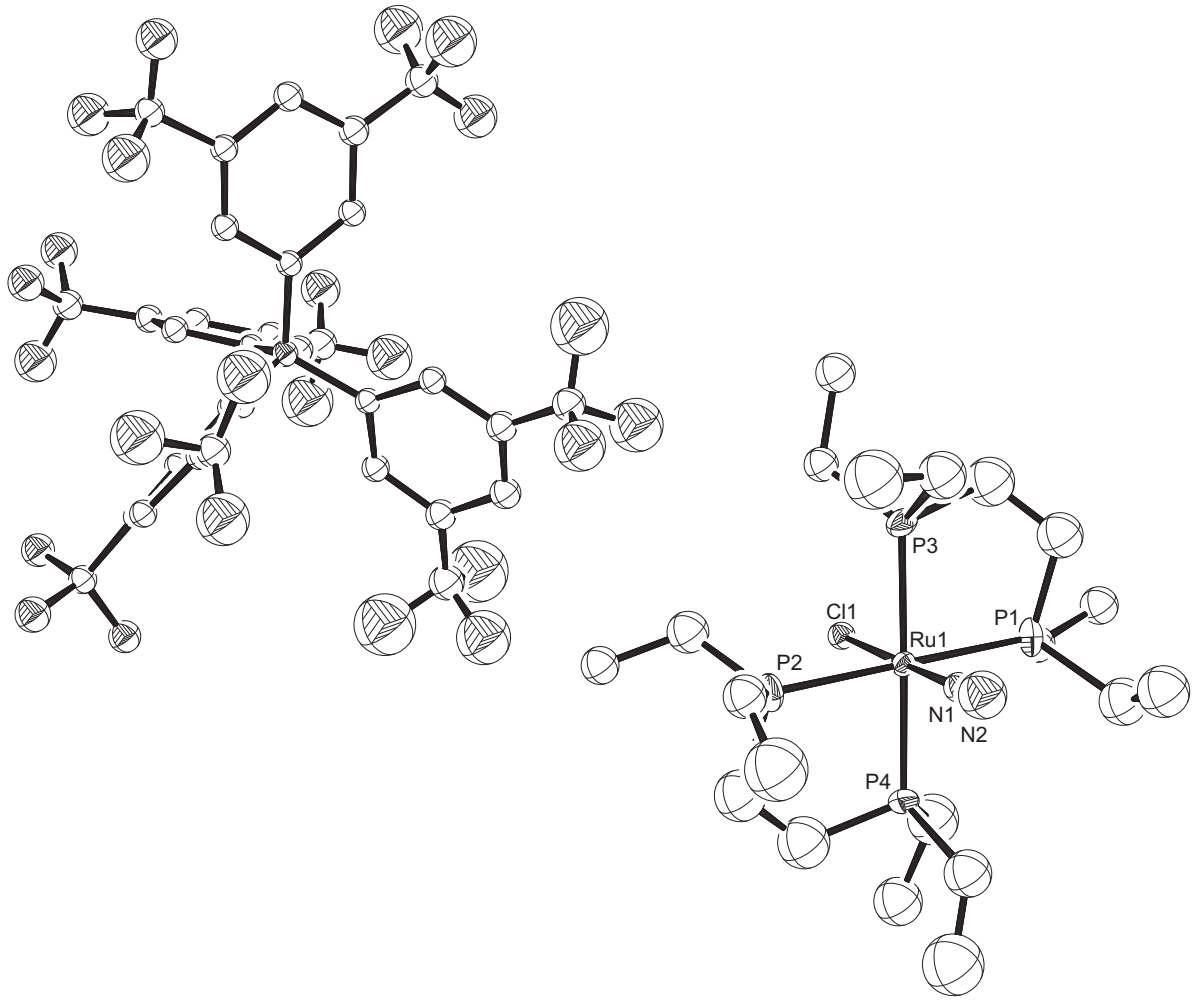

Figure 3.10 – ORTEP diagram of *trans*-$[RuCl(N_2)(depe)_2](BArF_{24})$ shown at 30% displacement ellipsoids. Hydrogen atoms omitted for clarity

An in depth analysis of the possible significance of structural dimensions for *trans*-$[RuCl(N_2)(depe)_2](BArF_{24})$ would not be justified in view of the crystal data, but several salient features nevertheless warrant mentioning, including that the Cl-Ru-N1 unit is essentially linear at 178.3°, and the N1-N2 bond length appears shorter (0.97 Å) than that observed in free dinitrogen.

Whilst it is unusual that the overall reaction has undergone two changes of geometry (from *trans*-[$RuCl_2(depe)_2$], to *cis*-[{$RuCl(depe)_2$}$_2(N_2)$]($BArF_{24}$), to *trans*-[$RuCl(N_2)(depe)_2$]($BArF_{24}$)), depe ligands are known to be labile[2] and weakly coordinating ligands such as dinitrogen may readily dissociate, thereby minimising the energy barrier associated with a change in geometry of the ruthenium *bis*-depe core.

The intermediate compound *cis*-[{$RuCl(depe)_2$}$_2(\mu\text{-}N_2)$]($BArF_{24}$) appears to be moderately stable, remaining unchanged in both d_4-methanol and d_8-thf solutions for at least one week, suggesting that the further reaction and isomerisation of this species to *trans*-[$RuCl(N_2)(depe)_2$]($BArF_{24}$) during crystallisation is either a function of solvent effects, with dichloromethane or heptane driving an equilibrium to the *trans* form, or of crystallisation itself, with the monomeric *trans* complex crystallising in preference to other species.

3.2.8 Treatment of *trans*-[$RuCl_2(depe)_2$] with $Tl(BF_4)$ in methanol

Reaction of *trans*-[$RuCl_2(depe)_2$] with thallium tetrafluoroborate in methanol heated at reflux resulted in the formation of copious amounts of a white precipitate together with a yellow solution that turned green upon filtration. Filtration through celite resulted in a significant loss of material that remained bound to the surface of the filtering agent, signifying a strongly ionic nature for the product.

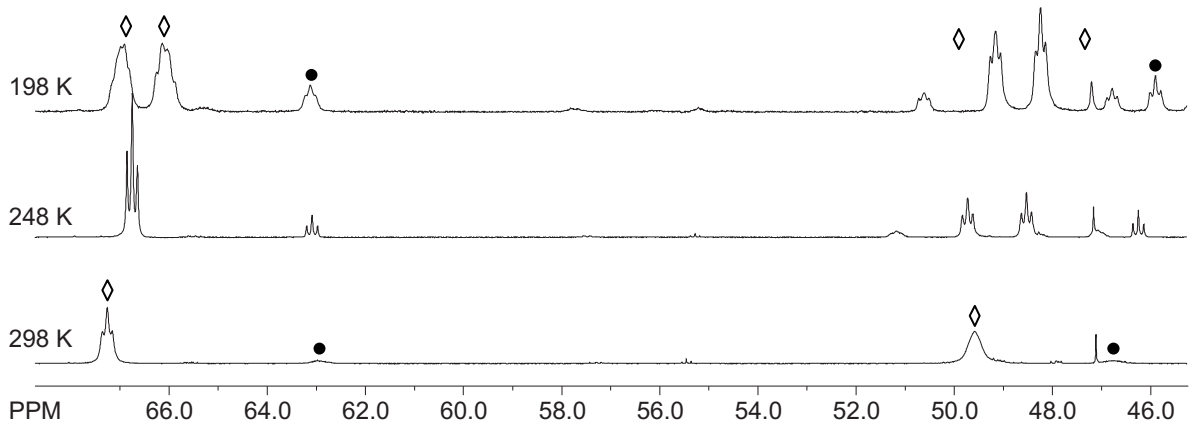

Figure 3.11 – Variable temperature $^{31}P\{^1H\}$ NMR spectra (d_8-thf, 202 MHz) of the product of the reaction of *trans*-$[RuCl_2(depe)_2]$ with $Tl(BF_4)$. ◊ – *cis*-$[RuCl(BF_4)(depe)_2]$; ● – *cis*-$[\{Ru(depe)_2\}_2(\mu\text{-}Cl)_2](BF_4)_2$

$^{31}P\{^1H\}$ NMR spectra of the reaction mixture are never completely sharp at temperatures above 198 K (inclusive), but reveal an ABMX spin system of an unusually fluxional, unsymmetrical *cis* complex (Figure 3.11). At 248 K, the equatorial phosphine resonances exhibit fast exchange on the NMR timescale, leading to the downfield resonances appearing as an apparent triplet. Further cooling slows this exchange to a rate which is intermediate on the NMR timescale and resolving the two non-equivalent equatorial positions. Thus, this species is assigned as *cis*-$[RuCl(BF_4)(depe)_2]$ in which there is rapid exchange between the equatorial positions (Scheme 3.4). Such exchange also prevents observation of fluorine-phosphine coupling.

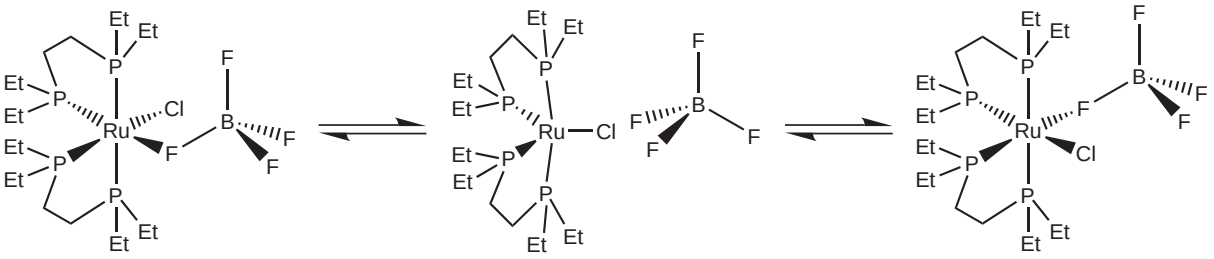

Scheme 3.3

MALDI-MS exhibits ion envelopes for $[RuCl(depe)_2]^+$, $[RuCl(N_2)(depe)_2]^+$, and an unknown ion at *m/z* 634, the latter having the same isotopic distribution and mass increase (85) over $[RuCl(depe)_2]^+$ that was observed in the analogous reaction with dmpe. Moreover, the IR spectrum reveals a moderate stretch at 2126 cm^{-1}. Nevertheless, whilst mass spectrometry and infrared spectroscopy are both suggestive of the formation of a dinitrogen complex, such a species is inconsistent with the NMR data. This discrepancy is ascribed to solution equilibria in tetrahydrofuran disfavouring the dinitrogen complex as the BF_4 anion, whilst binding only weakly in solution, successfully competes with dinitrogen as a ligand.

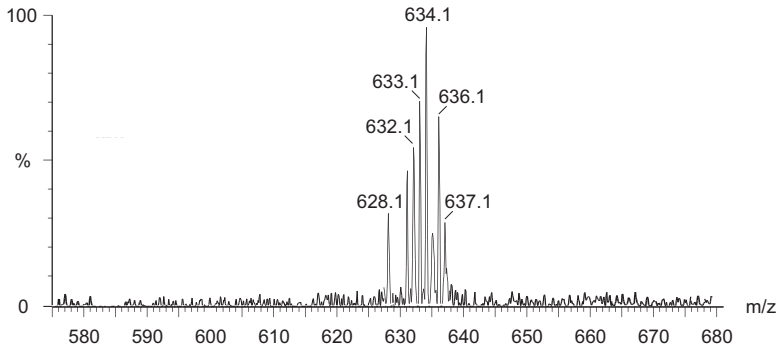

Figure 3.12 – MALDI-MS of the product from the reaction of *trans*-$[RuCl_2(depe)_2]$ with $Tl(BF_4)$ in methanol

3.3 Reactions of cis-*[$RuCl_2(depe)_2$]*

3.3.1 Treatment of *cis*-[$RuCl_2(depe)_2$] with TMS(OTf) in methanol

C*is*-[$RuCl_2(depe)_2$] was synthesised analogously to *cis*-[$RuCl_2(dmpe)_2$] (Chapter 2, Section 2.6.1).

The reaction of *cis*-[$RuCl_2(depe)_2$] with TMS(OTf) in methanol resulted in oxidation to [$RuCl_2(depe)_2$](OTf), with paramagnetically shifted ^{1}H alkyl resonances evident at 1.6, −9.7 and −13.2 ppm in the ^{1}H NMR spectrum. These chemical shifts are identical to those of *trans*-[$RuCl_2(depe)_2$](OTf) (Section 3.2.2) which suggests isomerisation of *cis*-[$RuCl_2(depe)_2$] upon oxidation (Scheme 3.4). This result contrasts with the analogous *cis*-[$RuCl_2(dmpe)_2$] reaction in which oxidation is avoided and a complex of the form *cis*-[RuCl(OTf)$(dmpe)_2$] is obtained (Chapter 2, Section 2.6.1).

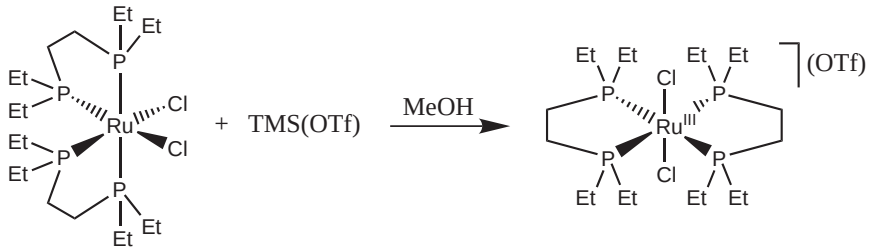

Scheme 3.4

3.3.2 Treatment of *cis*-$[RuCl_2(depe)_2]$ with $Tl(BArF_{24})$ in methanol

Reaction of *cis*-$[RuCl_2(depe)_2]$ with $Tl(BArF_{24})$ in methanol resulted in the rapid precipitation of a white solid. Filtration through celite followed by removal of the solvent *in vacuo* gave a yellow solid that slowly turned green under dinitrogen. The $^{31}P\{^1H\}$ NMR spectrum of the product reveals the presence of a non-fluxional, unsymmetrical *cis* complex (Figure 3.13), whilst MALDI-MS exhibits only one significant ion envelope at *m/z* 549, indicative of $[RuCl(depe)_2]^+$. A small ion envelope present at *m/z* 577 may possibly arise from a dinitrogen adduct, but this peak is barely above the noise floor and only the three largest isotope lines of ruthenium are visible. The IR spectrum exhibits no vibrations between 2550 and 1800 cm^{-1}, but the Raman spectrum possesses a strong signal at 2280 cm^{-1}. From the available data *cis*-$[\{RuCl(depe)_2\}_2)(\mu\text{-}N_2)](BArF_{24})_2$, a structure similar to that formed in the analogous *cis*-$[RuCl_2(dmpe)_2]$, is proposed (Scheme 3.5).

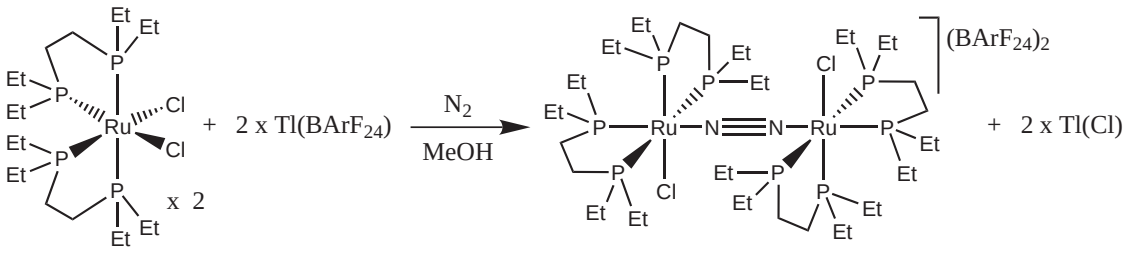

Scheme 3.5

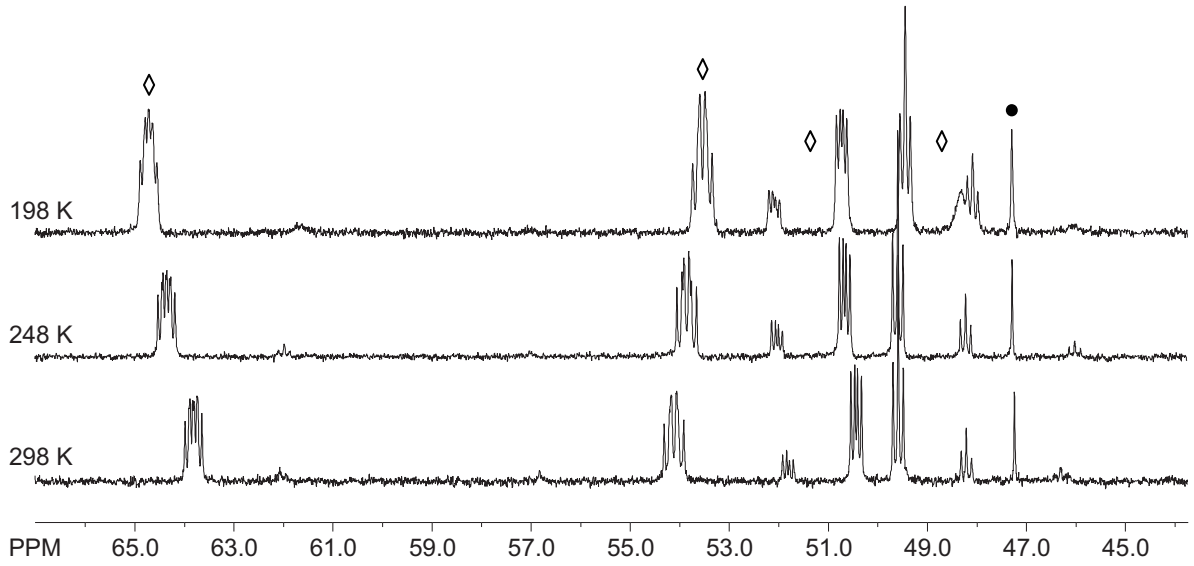

Figure 3.13 – Variable temperature $^{31}P\{^1H\}$ NMR spectra (d_8-thf, 202 MHz) of the reaction mixture of *cis*-$[RuCl_2(depe)_2]$ + $Tl(BArF_{24})$. ◊ – *cis*-$[\{RuCl(depe)_2\}_2)(N_2)](BArF_{24})_2$; ● – *trans*-$[RuCl_2(depe)_2]$

3.3.3 Treatment of *cis*-$[RuCl_2(depe)_2]$ with $Tl(BF_4)$ in methanol

Reaction of *cis*-$[RuCl_2(depe)_2]$ with $Tl(BF_4)$ in methanol heated at reflux produced a white precipitate and a red solution. Filtration through celite followed by solvent removal resulted in the isolation of a brick-red, solid film. The $^{31}P\{^1H\}$ NMR spectrum is complicated, containing multiple fluxional species (Figure 3.14). At ambient temperature, the spectrum exhibits two broad signals at 67 and 49 ppm, both of which have widths at half-height of greater than 100 Hz. Cooling the sample results in both of these broad resonances separating into three discrete signals. The system is still somewhat fluxional at 198 K, but identifiable are the products *cis*-$[RuCl(BF_4)(depe)_2]$ and *cis*-$[\{Ru(depe)_2\}_2(\mu\text{-}Cl)_2](BF_4)_2$, as

formed in the reaction of *trans*-$[RuCl_2(depe)_2]$ with thallium tetrafluoroborate (Section 3.2.8).

Also evident in the $^{31}P\{^1H\}$ NMR spectrum is an unidentified species with a downfield resonance that appears to be comprised of two overlapping triplets, and an upfield resonance that overlaps with the axial phosphine resonances of the unsymmetrical *cis* complex of which it is difficult to clearly observe the multiplicity.

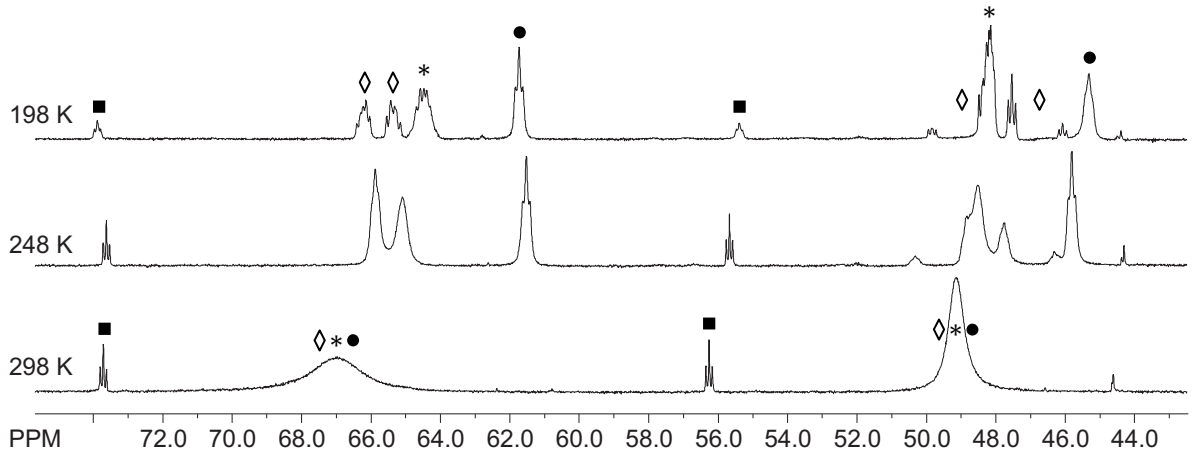

Figure 3.14 – Variable temperature $^{31}P\{^1H\}$ NMR spectra (d_8-thf, 202 MHz) of the reaction mixture of *cis*-$[RuCl_2(depe)_2]$ + $Tl(BF_4)$. ◊ – *cis*-$[RuCl(BF_4)(depe)_2]$; ● – *cis*-$[\{Ru(depe)_2\}_2(\mu\text{-}Cl)_2](BF_4)_2$; ■ – unknown *cis* symmetrical; * – unknown *cis* unsymmetrical

Whilst not strong, a small stretch at 2124 cm^{-1} in the IR spectrum may correspond to minor dinitrogen containing compound. Regular MALDI-MS contain only one ion envelope, corresponding to $[RuCl(depe)_2]^+$, although under extremely high laser power indistinct ion envelopes assignable as $[RuCl(N_2)(depe)_2]^+$ and $[Ru_2Cl_2(depe)_4]^+$ are visible.

Overall, the fluxional $^{31}P\{^1H\}$ behaviour evident in the $^{31}P\{^1H\}$ NMR spectra suggests that all three species are in exchange with one another and are, to an extent, similar in structure, which leads to a tentative assignment of the third species as *cis*-$[RuCl(N_2)(depe)_2]$. Why a dinitrogen complex should exist as an equilibrium species in this system and not the other reaction mixtures that exhibit the same *cis*-$[\{Ru(depe)_2\}_2(\mu\text{-}Cl)_2]^{2+}$ / *cis*-$[RuCl(depe)_2]^+$ pair is currently unknown, however in reaction mixtures which contain residual thallium salts, thallium may interact with the vacant ruthenium coordination site, preventing dinitrogen coordination.

3.4 Conclusions

As was observed for reactions of $[RuCl_2(dmpe)_2]$, the ruthenium(II) centre of $[RuCl_2(depe)_2]$ is prone to oxidation. Thus the reactions of TMS(OTf) with *trans*-$[RuCl_2(depe)_2]$ in toluene (Section 3.2.2) and *cis*-$[RuCl_2(depe)_2]$ in methanol (Section 3.3.1) resulted in formation of the ruthenium(III) complex *trans*-$[RuCl_2(depe)_2](OTf)$.

When oxidation was avoided, the reactions of *trans*-$[RuCl_2(depe)_2]$ were dominated by isomerisation to *cis* products, giving complexes identical to those formed from the analogous reactions of *cis*-$[RuCl_2(depe)_2]$. The most ubiquitous of these products was the chloride bridged dimeric ruthenium complex *cis*-$[\{Ru(depe)_2\}_2(\mu\text{-}Cl_2)](X)_2$ (X = OTf, BF_4). This

complex was observed to be stabilised by both thallium(I) (Section 3.2.3) and silver(I) (Section 3.2.6), although it also existed stably without additional cations (Section 3.2.5). The formation of such a dimer is in contrast to the analogous reactions of $[RuCl_2(dmpe)_2]$ (Chapter 2), where *cis*/*trans* isomerisation was rarely seen and dimeric structures not at all, with anion coordination observed in preference. For $[RuCl_2(depe)_2]$ however, even the reactions of $Tl(BF_4)$ with *trans*- and *cis*-$[RuCl_2(depe)_2]$ (Sections 3.2.8 and 3.3.3 respectively) resulted in formation of minor amounts of dimeric *cis*-$[\{Ru(depe)_2\}_2(\mu\text{-}Cl_2)](BF_4)_2$ in addition to *cis*-$[RuCl(BF_4)(depe)_2]$ as their major product.

In a manner similar to the reactions of $[RuCl_2(dmpe)_2]$ discussed in Chapter 2, the only unequivocal dinitrogen-containing complexes formed from $[RuCl_2(depe)_2]$ result from reactions involving the $BArF_{24}$ anion. Chloride abstractions from *trans*- and *cis*-$[RuCl_2(depe)_2]$ using $Tl(BArF_{24})$ (Sections 3.2.7 and 3.3.2 respectively) resulted in formation of the dinitrogen-bridged dimeric complex *cis*-$[\{RuCl(depe)_2\}_2(\mu\text{-}N_2)](BArF_{24})$, directly analogous to the dmpe complex *cis*-$[\{RuCl(dmpe)_2\}_2(\mu\text{-}N_2)](BArF_{24})$ (Chapter 2, Section 2.6.2). The dinitrogen-bridged dimer was observed to further take up N_2, crystallising as the terminal dinitrogen complex *cis*-$[RuCl(N_2)(depe)_2](BArF_{24})$, which suggests that dinitrogen solubility in organic solvents may be a limiting factor in this reaction.

References

1. Hughes, D. L.; Leigh, G. J.; Jimenez-Tenorio, M.; Rowley, A. T., J. *Chem. Soc., Dalton Trans.* **1993**, (1), 75-82.

2. Baker, M. V.; Field, L. D.; Hambley, T. W., *Inorg. Chem.* **1988,** 27, (16), 2872-2876.

3. Bruce, M. I., *Angew. Chem., Int. Ed. Engl.* **1977,** 16, (2), 73-86.

4. Forsén, S.; Hoffman, R. A., J. *Chem. Phys.* **1963,** 39, (11), 2892-2901.

5. Jeener, J.; Meier, B. H.; Bachmann, P.; Ernst, R. R., J. *Chem. Phys.* **1979,** 71, (11), 4546-4553.

6. Garrou, P. E., *Inorg. Chem.* **1975** 14, (6), 1435-1439.

7. Drouin, S. D.; Foucault, H. M.; Yap, G. P. A.; Fogg, D. E., *Organometallics* **2004,** 23, (11), 2583-2590.

8. Bickley, J. F.; Higgins, S. J.; Stuart, C. A.; Steiner, A., *Inorg. Chem. Comm.* **2000,** 3, (5), 211-213.